Analytical approximation for post-shock physical conditions in the type II supernova shells

D.K. Nadyozhin[1,2], A.Yu. Deputovich[1]
[1] *Institute of Theoretical and Experimental Physics, Moscow, Russia*
[2] *Max-Planck-Institut für Astrophysik, Garching, Germany*

Abstract

We describe simple analytical formulae constructed to approximate the temporal behavior of the temperature, density, and radius of various presupernova shells immediately after the arrival of the supernova shock wave. The formulae are derived from detailed hydrodynamical simulation of the supernova envelope expulsion. When used in the traditional nuclear kinetic codes, the formulae are expected to be useful tool for adjusting the resulting nuclear yields to current supernova models.

Introduction

A considerable progress in the theory of stellar nucleosynthesis (see [1] for a comprehensive review) stirred up an ever increasing interest of astrophysicists and especially nuclear physicists in the modelling of nuclear processes in stars, in general, and in supernovae, in particular. It would be very useful to have at hand simple analytical approximations describing the physical conditions in the supernova shells heated and accelerated by the shock wave (SW). The purpose of the present paper is to show that such a goal can be achieved, at least for supernovae of Type II (and of Types Ib, Ic as well). In these supernovae, the hydrodynamics of the envelope expulsion is virtually insensitive to the details of the supernova mechanism generating a powerful SW at the interface between the collapsing iron core and outer envelope finally to be expelled. The only meaningful parameter connecting the explosion mechanism and envelope outburst is the total explosion energy E. On the contrary in the case of the Type Ia supernovae, one cannot disentangle the explosive thermonuclear burning from the hydrodynamics of the expulsion which ultimately all the stellar matter turns out to be drawn in.

In the following sections, first we describe briefly the hydrodynamic simulation of the Type II supernova explosions and then derive analytical approximations for the temporal behavior of the temperature, density and radius of shocked matter in different shells of

$15\,\mathrm{M}_\odot$ and $30\,\mathrm{M}_\odot$ supernova models. In particular, we show that a simple exponential approximation used widely for the post-shock temperature: $T \sim \exp[-t/(3\tau)]$ where τ is the "hydrodynamic" time scale connected with the *local* pre-shock density ρ by the expression

$$\tau = \frac{446}{\sqrt{\rho}}\ \mathrm{s}\,, \tag{1}$$

is actually far from to be satisfactory.

The preliminary results of this study were reported at the 10th Ringberg Castle Workshop on Nuclear Astrophysics [2].

Hydrodynamic simulation

In order to obtain the approximation of the supernova SW properties useful for exploring nucleosynthesis, we have fulfilled a series of supernova hydrodynamic simulations. The calculations were done with the aid of the hydrodynamic supernova code SNV used long ago at ITEP (see, e.g. [3]). The code was run in its simplest mode that realizes an explicit difference scheme for adiabatic hydrodynamics with the artificial viscosity being utilized to control the propagation of shock waves. There was used the equation of state EPEOS from [4] that took into account the black-body radiation and full Fermi–Dirac statistics for the electron-positron component. This last point turns out to be of importance for the SW properties in the SiS- and CO-shells where the number of the electron-positron pairs can become comparable with the number of "atomic" electrons [5].

Two Woosley–Weaver presupernova models of $15\,\mathrm{M}_\odot$ and $30\,\mathrm{M}_\odot$ [6] were taken as initial conditions. The two models have the red supergiant structure of radii $490\,\mathrm{R}_\odot$ and $1025\,\mathrm{R}_\odot$, and iron cores of $1.4\,\mathrm{M}_\odot$ and $1.85\,\mathrm{M}_\odot$, respectively. They have rather complicated chemical structure. For our aim, it seems to be adequate to divide each model into three shells of special importance for nucleosynthesis: silicon-sulfur (SiS), carbon-oxygen (CO, for $15\,\mathrm{M}_\odot$), or oxygen (O, for $30\,\mathrm{M}_\odot$), and helium (He) one. Tables 1 and 2 summarize the properties of the onion-like shell structure of these models.

The supernova outburst was simulated through the initial conditions by instantaneous liberation of the explosion energy E in a narrow mass layer ($\delta m \approx 0.1\,\mathrm{M}_\odot$) located just at the outer boundary of the iron core, below the SiS-shell. The bottom of this layer was considered in the internal boundary condition as a rigid wall at rest where the velocity remained equal to zero all the time. Several modes of the energy release (with different proportion of thermal to kinetic energy component) have been tested in the preliminary calculations to make sure that our results are independent of the specific way of energy release.

Table 1 : The shell structure of a 15 $M_\odot$ presupernova.

Shell	$m\,(M_\odot)$	$R_0\,(10^8\,\mathrm{cm})$	$\rho_0\,(\mathrm{g\,cm^{-3}})$	$T_0\,(\mathrm{K})$
SiS-bottom	1.43	1.51	$2.18{\cdot}10^7$	$4.73{\cdot}10^9$
SiS-middle	1.53	1.90	$1.03{\cdot}10^7$	$3.84{\cdot}10^9$
SiS-top & CO-bottom	1.63	2.31	$5.28{\cdot}10^6$	$3.33{\cdot}10^9$
CO-middle	2.19	8.72	$1.29{\cdot}10^5$	$1.12{\cdot}10^9$
CO-top & He-bottom	2.75	34.3	$1.05{\cdot}10^3$	$2.82{\cdot}10^8$
He-middle	3.60	161	$3.17{\cdot}10^1$	$7.74{\cdot}10^7$
He-top & HHe-bottom	4.45	550	$2.12{\cdot}10^{-1}$	$1.46{\cdot}10^7$

Table 2 : The shell structure of a 30 $M_\odot$ presupernova.

Shell	$m\,(M_\odot)$	$R_0\,(10^8\,\mathrm{cm})$	$\rho_0\,(\mathrm{g\,cm^{-3}})$	$T_0\,(\mathrm{K})$
SiS-bottom	1.88	2.47	$9.43{\cdot}10^6$	$3.96{\cdot}10^9$
SiS-middle	2.11	3.17	$4.48{\cdot}10^6$	$3.28{\cdot}10^9$
SiS-top & O-bottom	2.32	3.97	$2.41{\cdot}10^6$	$2.71{\cdot}10^9$
O-middle	5.77	28.1	$2.69{\cdot}10^4$	$8.20{\cdot}10^8$
O-top & He-bottom	9.20	67.7	$7.46{\cdot}10^2$	$3.07{\cdot}10^8$
He-middle	10.5	140	$1.02{\cdot}10^2$	$1.51{\cdot}10^8$
He-top & HHe-bottom	11.8	547	$7.72{\cdot}10^{-2}$	$1.82{\cdot}10^7$

Analytical approximations

To begin with constructing the approximation formulae, first we have to specify the main parameters determining the temporal behavior of shocked matter. They are: the energy of the explosion E which comes from the supernova mechanism unfortunately not yet known in detail, the identity of the shell under consideration (SiS, CO, He), the initial (pre-shock) density ρ_0 and radius R_0 of the shell. The initial temperature T_0 of the shell is virtually unimportant since the SW is always very strong.

The second step is to find out such combinations of these parameters which could serve as useful units to measure the post-shock temperature T_p and time t. The best candidate for the temperature unit is the Weaver–Woosley estimate for the SW peak temperature [7]. This temperature, that we designate as T_{WW} , is equal to the temperature of the black-body radiation which uniformly fills the sphere of the SW radius R_0 and has total energy equal to the supernova explosion energy E: $\frac{4\pi}{3} R_0^3\, aT_{\rm WW}^4 = E$. So, $T_{\rm WW}$ scales as $E^{0.25} R_0^{-0.75}$ and reproduces the SW peak temperature T_p with a good accuracy (within $\pm 20\%$) along all the SW way through presupernova shell structure [5].

An appropriate estimate of the characteristic time t_u can be drawn from the following consideration. The time scale of the post-shock expansion is controlled by the speed of sound, $v_{\rm sound}$, in shocked matter and by the order of magnitude is equal to $t_u = R_0/v_{\rm sound}$. Taking into account that $v_{\rm sound}^2 = \gamma P/\rho$, one can obtain that $v_{\rm sound} \sim 1/\sqrt{\rho}$ for the radiation dominated media where $\gamma = 4/3,\ P = aT^4/3$. We see that dependence of the characteristic time t_u on density turns out to be just opposite to that for τ from Eq. (1). Such a correct way to estimate the time scale of the post-shock expansion was used earlier in ref. [8]. The final expressions for $T_{\rm WW}$ and t_u are

$$T_{\rm WW} = \left(\frac{3E}{4\pi a R_0^3}\right)^{1/4} = 2.37\cdot 10^9\ E_{51}^{0.25} \left(R_0/10^9\,{\rm cm}\right)^{-0.75}\ {\rm K}\,, \tag{2}$$

$$t_u = 3.83\cdot 10^{-3}\, \rho_0^{0.5} E_{51}^{-0.5} \left(R_0/10^9\,{\rm cm}\right)^{2.5}\ {\rm sec}\,, \tag{3}$$

where $E_{51} \equiv E/10^{51}$ erg. The above expression for $t_u = R_0/v_{\rm sound}$ was obtained by using $P = aT_{\rm WW}^4/3$, $\gamma = 4/3$, and $\rho = 7\rho_0$ for the post-shock pressure, adiabatic index, and density.

The natural units of length and density are the initial radius R_0 and pre-shock density ρ_0 of the layer crossed over by the SW.

In terms of the above units, the results of our hydrodynamic calculations for different supernova layers of a 15 $M_\odot$ and 30 $M_\odot$ models can be approximated by the following simple relations for the temporal evolution of temperature, density, and radius of a Lagrangian layer:

$$T(t) = \frac{T_p}{1+\xi_T\, t/t_u}\,, \quad T_p = \xi_p\, T_{\rm WW}\ , \tag{4}$$

$$\rho(t) = \rho_p \left(\frac{T}{T_p}\right)^3, \quad \rho_p = 7\rho_0\,, \tag{5}$$

$$R(t) = R_0\,(1+\xi_r t/t_u)\,, \tag{6}$$

where T_p and ρ_p are the peak temperature and density of shocked matter while ξ_p, ξ_T, and ξ_r are the dimensionless structural coefficients chosen to fit the hydrodynamic calculations as close as possible.

Equations (4–6) imply that the SW reaches the layer at $t = 0$.

In the case of the neutrino nucleosynthesis (see, e.g. [9]), one has to take into account that the neutrino flux scales as $L_\nu(t+\delta t_{SW}+\Delta t_{SW})/R^2(t)$ where L_ν is the partial[1] neutrino luminosity, Δt_{SW} is the total time takes SW to reach the layer under consideration, whereas δt_{SW} is the time interval between the beginning of the neutrino burst and the moment of the SW transition from a steady accreting state into an outgoing blast wave; δt_{SW} depends on supernova mechanism (typically $\delta t_{SW} \approx 0.1$ sec).

[1]related to those types of neutrino which actually take part in nucleosynthesis

The values of Δt_{SW}, obtained in our hydrodynamical calculations, can be approximated with an accuracy of $\approx 20\%$ by the following formula:

$$\Delta t_{SW} = \xi_{SW}\, E_{51}^{-0.38} \left(R_0/10^9\mathrm{cm}\right)^{1.4} \mathrm{sec}\,, \tag{7}$$

where ξ_{SW} is another dimensionless fitting coefficient.

The numerical values of the above fitting coefficients are presented in Tables 3 and 4 for different layers of 15 $\mathrm{M}_{\odot}$ and 30 $\mathrm{M}_{\odot}$ supernovae.

Table 3: The structural coefficients for a 15 $\mathrm{M}_{\odot}$ supernova.

Shell	ξ_p	ξ_T, (ξ_{T1})	ξ_r, (ξ_{r1}, ξ_{r2})	ξ_{SW}
SiS-middle	1.1	2.2, (13)	1.1, (0.5, 2.2)	0.54
SiS-top & CO-bottom	1.1	2.2, (13)	1.1, (0.5, 2.2)	0.74
CO-middle	0.95	1.4	1.25	1.10
CO-top & He-bottom	0.85	0.90	0.85	0.98
He-middle	0.90	1.5	1.3	0.69
He-top & HeH-bottom	0.75	1.3	1.1	0.54

Table 4: The structural coefficients for a 30 $\mathrm{M}_{\odot}$ supernova.

Shell	ξ_p	ξ_T, (ξ_{T1})	ξ_r, (ξ_{r1}, ξ_{r2})	ξ_{SW}
SiS-middle	1.07	1.4, (8.0)	1.0 (0, 4.5)	0.36
SiS-top & O-bottom	1.0	1.3, (6.0)	1.0 (0, 4.5)	0.49
O-middle	0.80	2.0	1.1	1.52
O-top & He-bottom	0.80	1.1	0.90	1.40
He-middle	0.80	1.3	1.1	1.18
He-top & HeH-bottom	0.80	1.0	1.0	0.58

We did not present the approximations for the bottom of the SiS-shell. The reason is that this layer is very close to the place of explosive energy release and hydrodynamical flow still can remember the details of the artificial initial conditions used in our calculations.

Figures 1–22 show the temporal evolution of the post-shock temperature and radius for both the models (15 $\mathrm{M}_{\odot}$ and 30 $\mathrm{M}_{\odot}$). The results of our hydrodynamic calculations are shown in each figure by a bunch of full lines related to a wide range of the supernova explosion energies covered in our calculations: $1 \cdot 10^{51} \lesssim E \lesssim 2 \cdot 10^{52}$ erg. The dashed lines demonstrate the approximations given by Eqs. (4) and (6) for the temperature and radius, respectively.

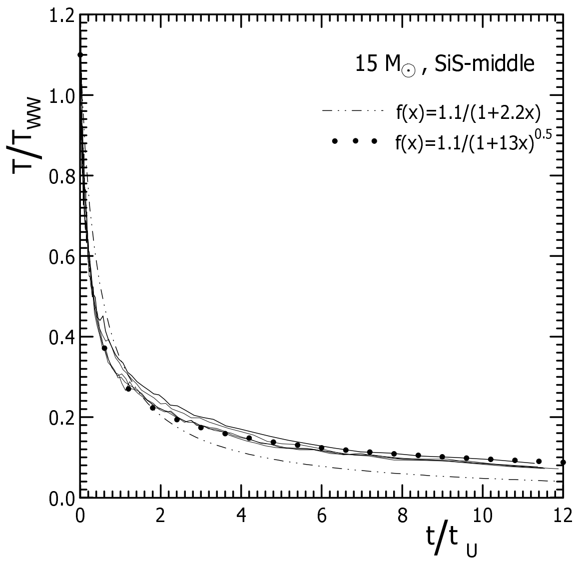

Figure 1

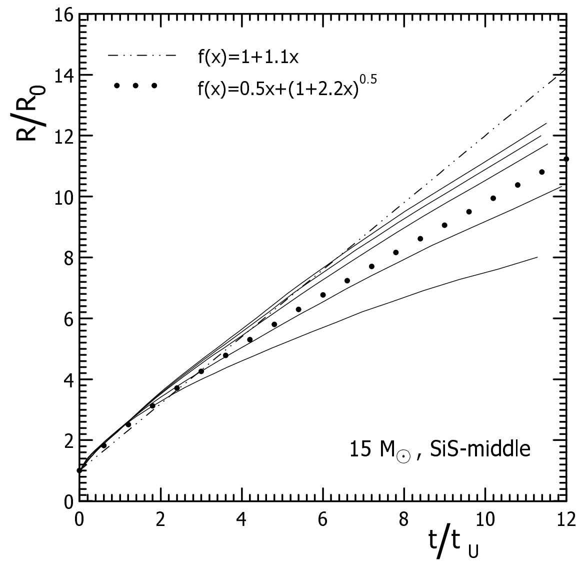

Figure 2

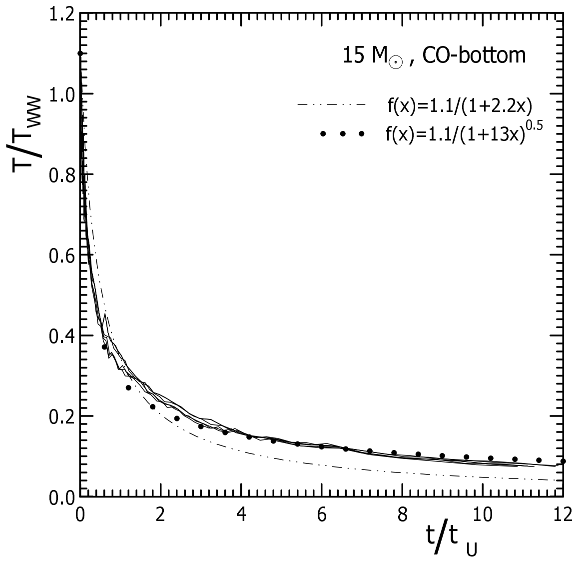

Figure 3

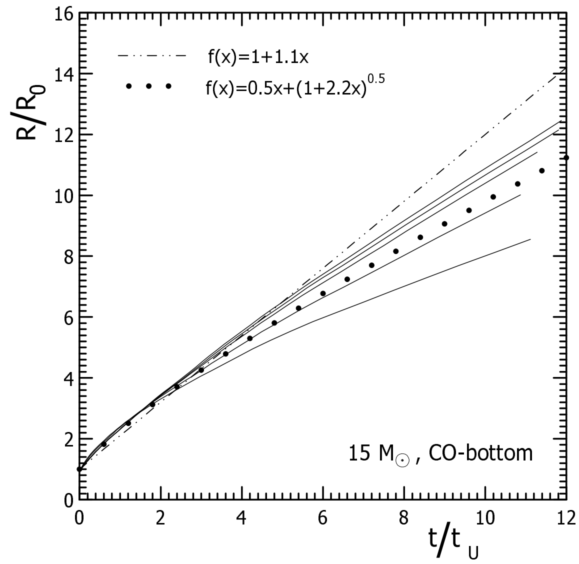

Figure 4

Looking these figures through one can ascertain a good coincidence between the approximations and hydrodynamic calculations. When finding the best values for the structural coefficients, we have focused our attention on the time interval $0 \leq t/t_u \lesssim 2$ because the later times ($t/t_u \gtrsim 2$) prove to be of a minor (if any) importance for nucleosynthesis since the temperature falls down by a factor of 4–5 as compared with its peak value. From this point of view, the temperature approximation, for instance, in Fig. 7 could be considered nearly as good as that in Fig. 5. There is, however, a certain doubt about the quality of the approximation in the middle and the top of the SiS-shell — look at Figs. 1–4 for a $15\,\mathrm{M}_\odot$ model and Figs. 13–16 for a $30\,\mathrm{M}_\odot$ model (we remind that the top of the SiS-shell coincides with the bottom of CO-shell for a $15\,\mathrm{M}_\odot$ model and that of O-shell for a $30\,\mathrm{M}_\odot$ model). Although Eqs. (4) and (6) could nevertheless be useful as the first guess for the SiS-shell, the following approximate formulae for $T(t)$ and $R(t)$ turn out to be much more accurate:

$$T(t) \;=\; \frac{T_p}{\sqrt{1+\xi_{T1}\,t/t_u}}\,, \quad T_p \;=\; \xi_p\,T_{\mathrm{WW}}\;, \tag{8}$$

$$R(t) \;=\; R_0\left(\xi_{r1}\,t/t_u + \sqrt{1+\xi_{r2}\,t/t_u}\right). \tag{9}$$

The structural coefficients ξ_{T1}, ξ_{r1}, and ξ_{r2} are given in parenthesis in Tables 3 and 4. These approximations are shown in Figs. 1–4, 13–16 by black dots (not connected by lines!). One can see an excellent agreement for the temperature curves and a fairly good one for the radius curves.

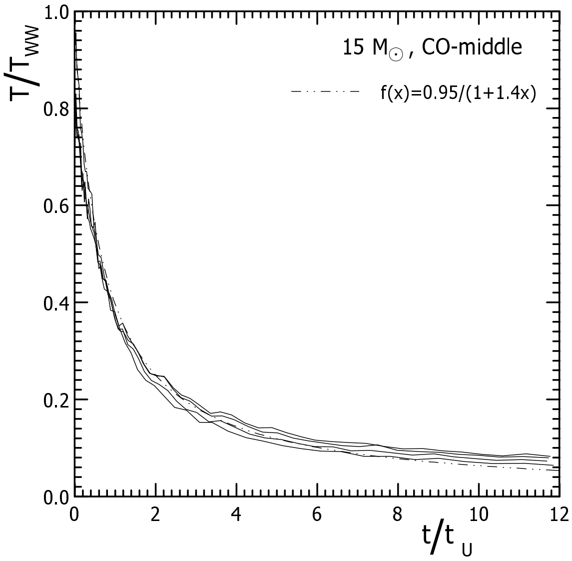

Figure 5

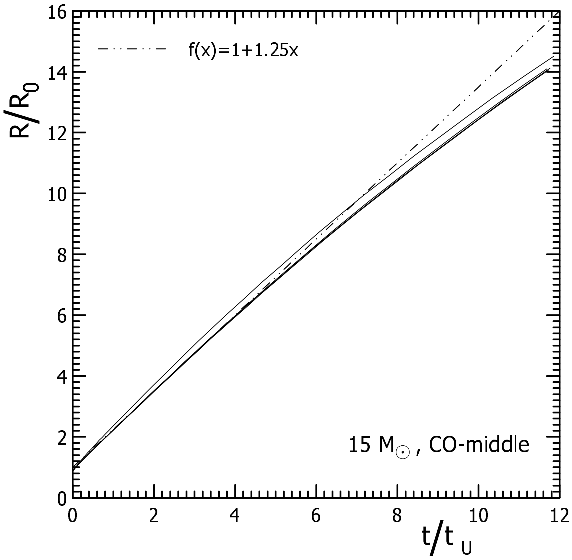

Figure 6

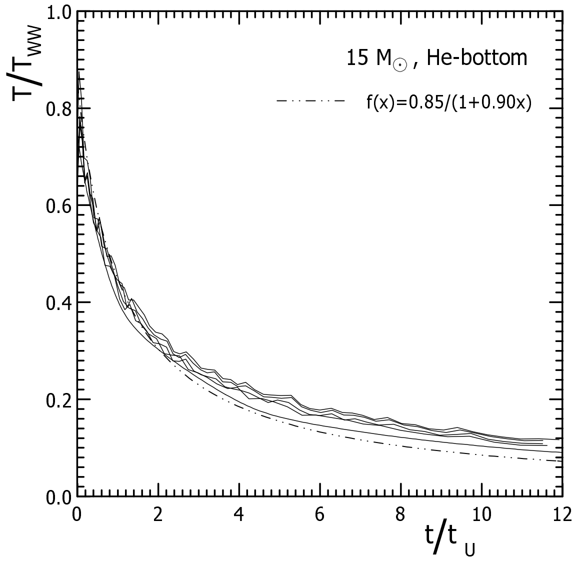

Figure 7

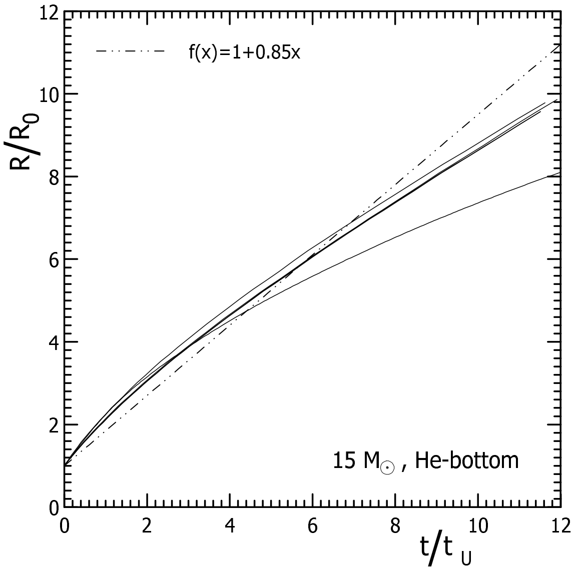

Figure 8

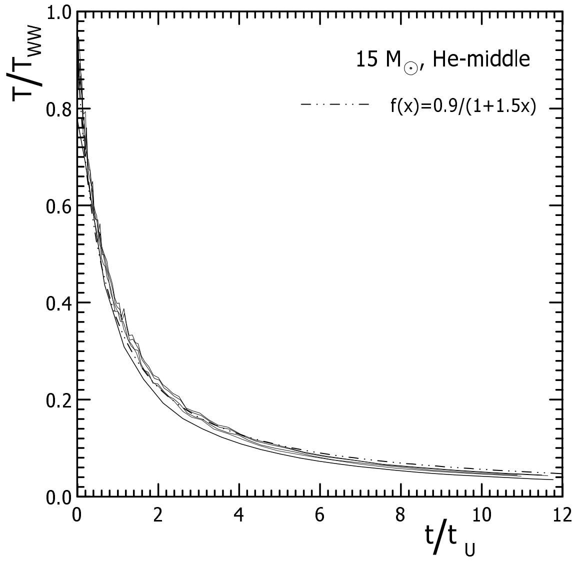

Figure 9

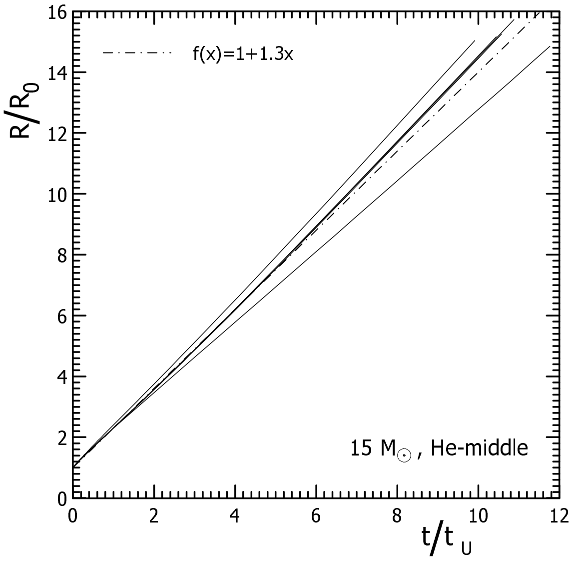

Figure 10

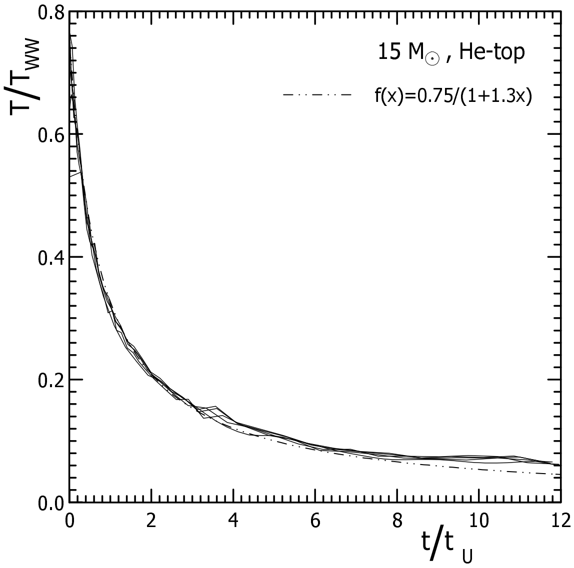

Figure 11

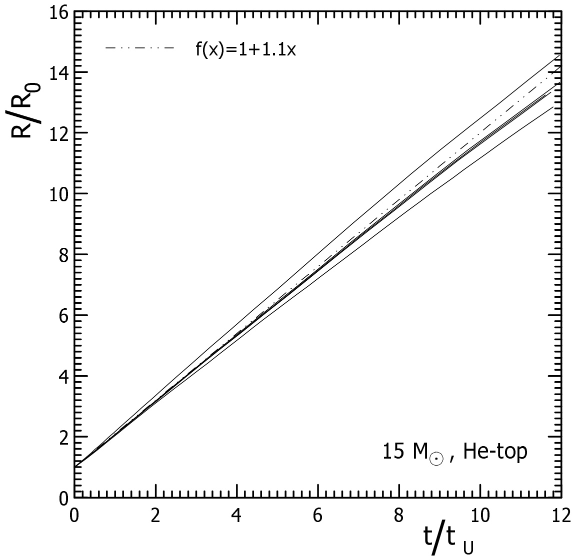

Figure 12

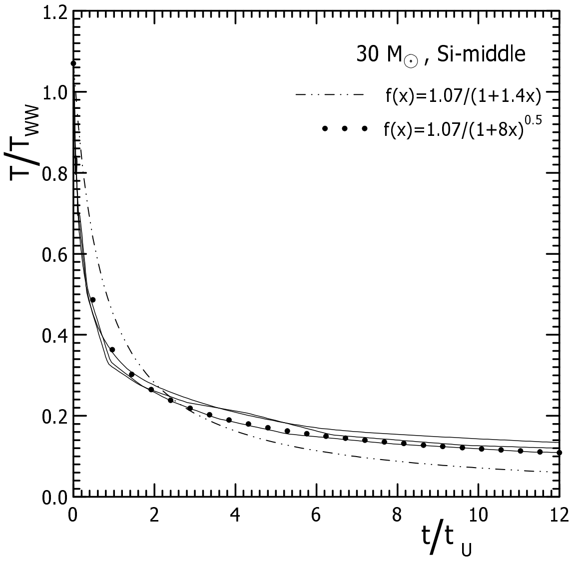

Figure 13

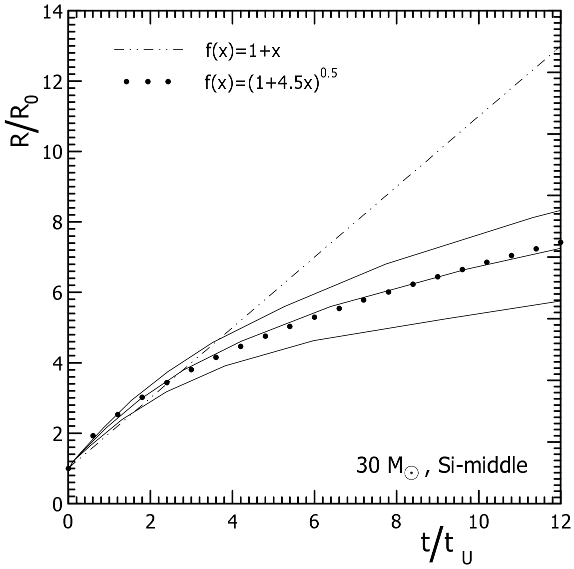

Figure 14

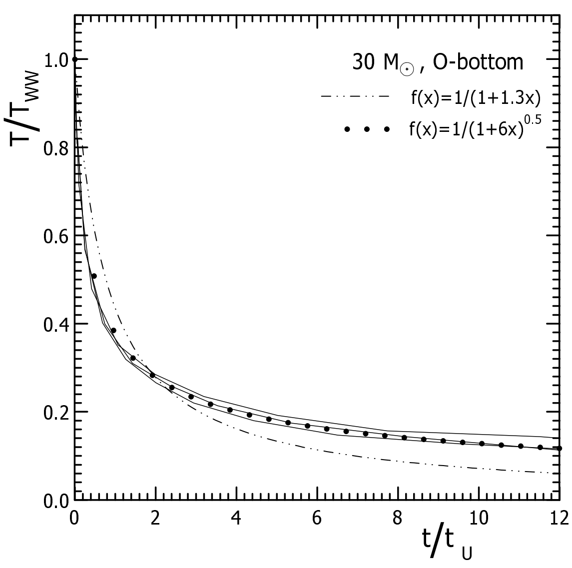

Figure 15

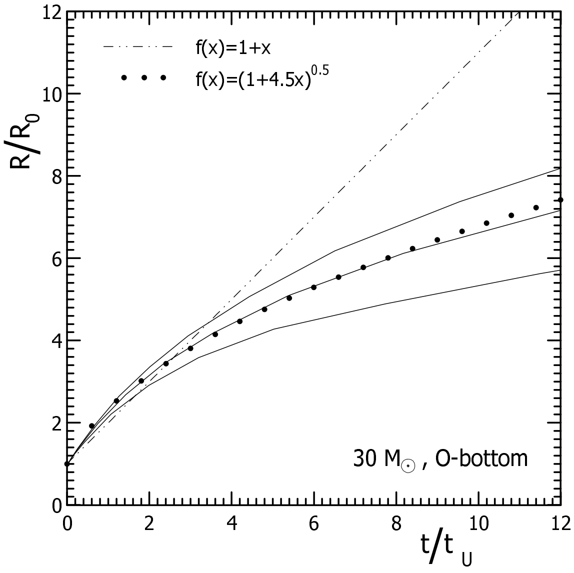

Figure 16

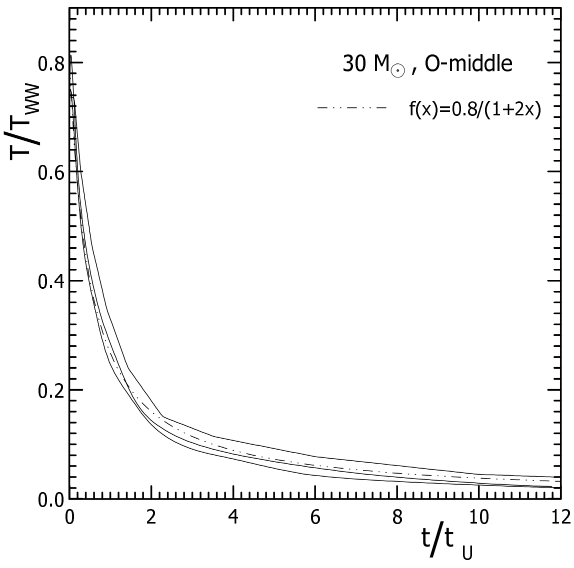

Figure 17

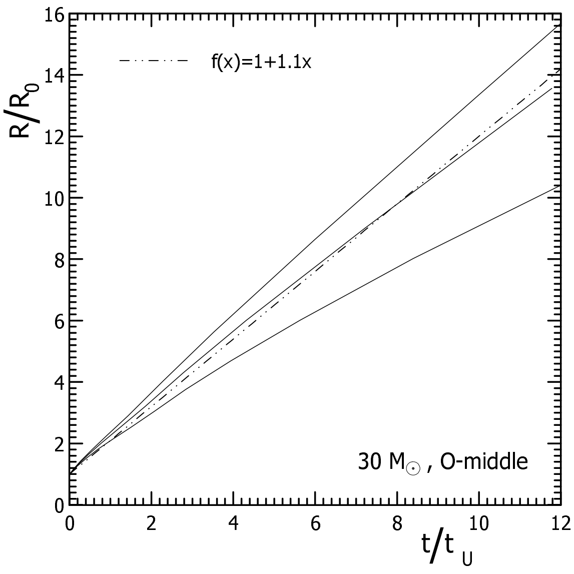

Figure 18

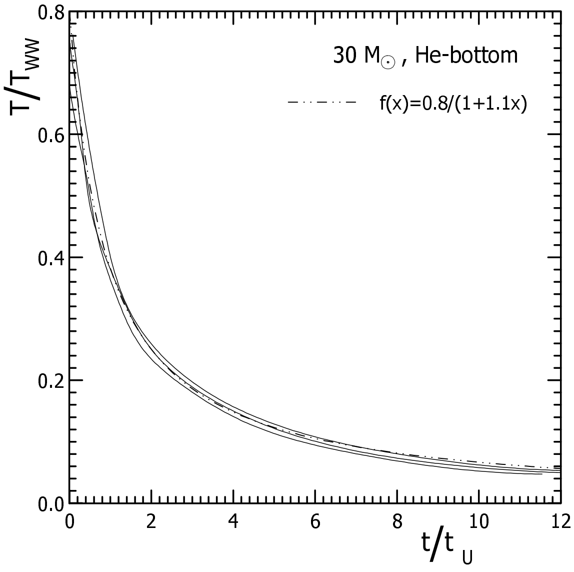

Figure 19

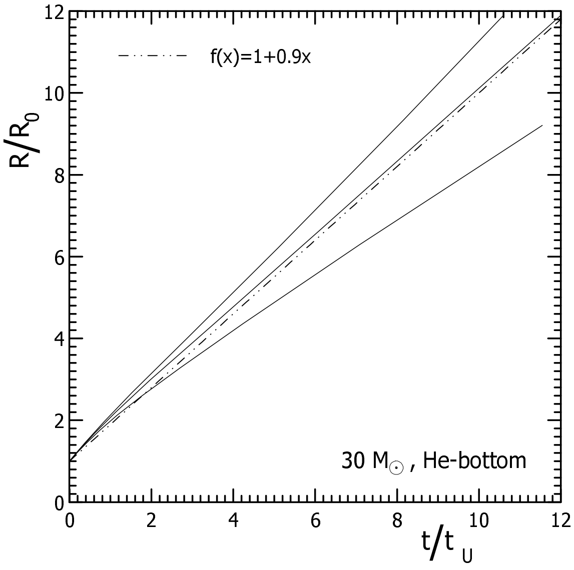

Figure 20

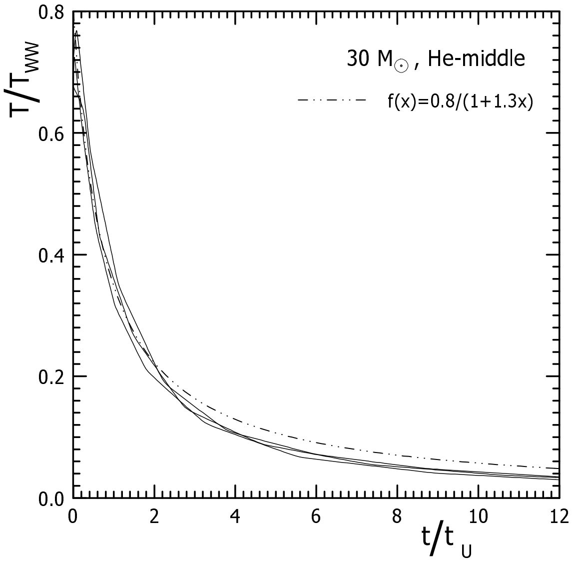

Figure 21

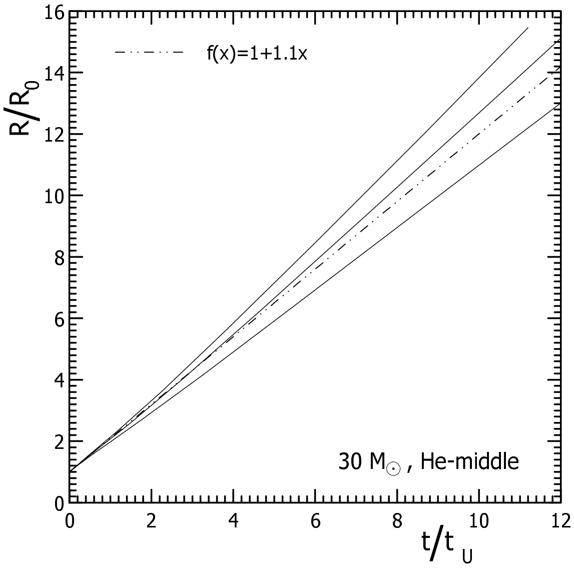

Figure 22

Figures 23 and 24 demonstrate that the exponential approximation based on the "hydrodynamic" time scale τ (Eq. 1) is not actually adequate. It predicts a much slower decrease in the post-shock temperature, even when one uses the peak density $\rho_p = 7\rho_0$ to evaluate τ (the curves labelled by number 2 in Figs. 23 and 24) rather than the initial pre-shock density ρ_0 (the curves labelled by 1). The discrepancy is especially pronounced for the helium shell (Fig. 24). The curves 1 and 2 in Figs. 23 and 24 are drawn for a standard explosion energy $E = 1.5 \cdot 10^{51}$ erg.

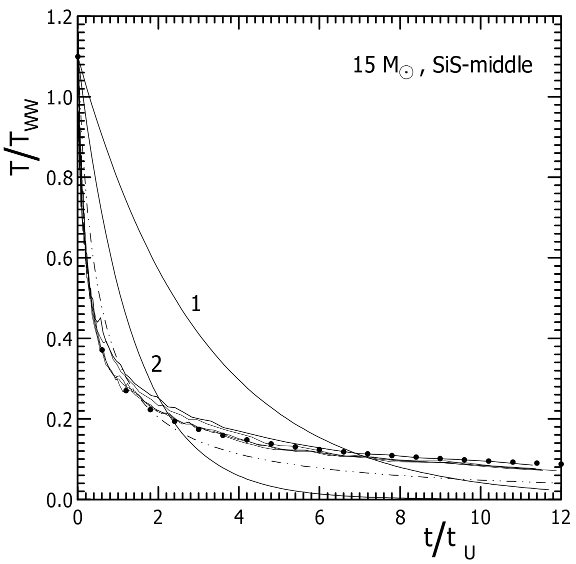

Figure 23: The comparison of the post-shock temperature in the middle of SiS-shell with a simplified "hydrodynamic" approximation shown by curves 1 and 2 (see text).

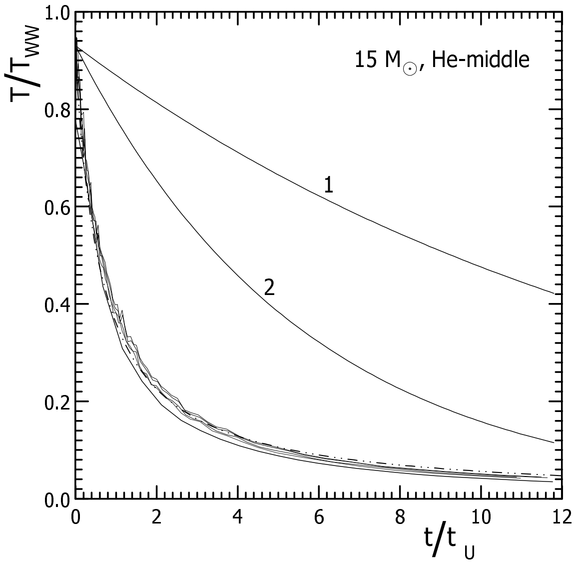

Figure 24: Same as in Fig. 23 but in the middle of He-shell.

It remains to discuss the approximation for density given by Eq. (5). Since the density is not so very important for nucleosynthesis as the temperature, the acceptable approximation should not be necessarily of a high accuracy. From this point of view Eq. (5) can serve as an appropriate approximation.

In Table 5, one can find the numerical values of the parameters involved in our consideration in the case of standard supernova explosion energy $E = 1.5 \cdot 10^{51}$ erg. The SW compression ρ_p/ρ_0 given in the last column of Table 5 was calculated from the Hugoniot conditions using corresponding values of T_p (the third column) and ρ_0 (from Tables 1 and 2). One can see that the approximation $\rho_p/\rho_0 = 7$ is not very far from reality. Still we have to verify how the assumption $\rho(t) \sim T^3(t)$ does actually work. Figure 25 shows the divergence F_ρ of actual $\rho(t)$ from the approximation given by Eq. (5):

$$\mathrm{F}_\rho = \frac{\rho(t)}{\rho_p} \left(\frac{T_p}{T}\right)^3 , \tag{10}$$

where the "isentropic" density $\rho(t)$ is calculated from the condition that entropy remains constant in every Lagrangian layer during its post-shock expansion: $S[\rho, T(t)] = S(\rho_p, T_p) = S_p = \text{const}$. Here S_p is the SW peak entropy and $T = T(t)$ is defined either by Eq. (4) or (8). If $\rho(t)$ followed strictly the law $\rho \sim T^3$, F_ρ would remain all the time equal to 1. We see that for a 15 M$_\odot$ model the declination from this law is virtually insignificant — it remains in the limits $\pm 30\%$. However in the He- and O-shell of a 30 M$_\odot$ model the "isentropic" density is decreasing more slowly than T^3. Nevertheless, the approximation $\rho \sim T^3$ still could be acceptable even in the O-shell of a 30 M$_\odot$ model if one remembered that nucleosynthesis occurs efficiently in the time interval $0 \leq t/t_u \lesssim 2$ — by the moment

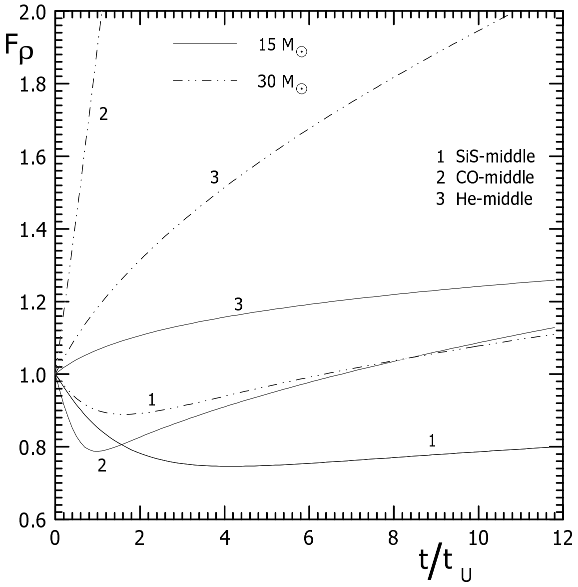

Figure 25: The divergence of the post-shock density from the approximation given by Eq. (5).

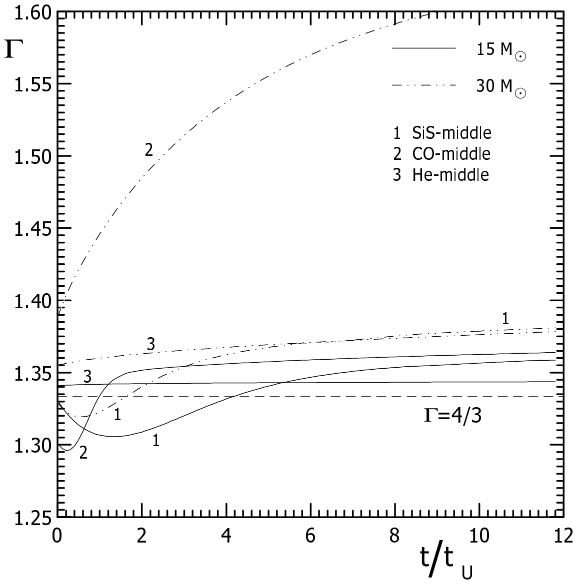

Figure 26: Adiabatic index Γ versus time for the post-shock expansion. The level $\Gamma = 4/3$ is shown by a horizontal dashed line.

Table 5: The shock wave parameters for a 15 $M_\odot$ and 30 $M_\odot$ supernovae with the explosion energy $1.5 \cdot 10^{51}$ erg.

Shell	M ($M_\odot$)	T_p (K)	T_{WW} (K)	t_u (sec)	Δt_{SW} (sec)	ρ_p/ρ_0
SiS-middle	15	$1.00 \cdot 10^{10}$	$9.10 \cdot 10^{9}$	0.158	$4.53 \cdot 10^{-2}$	6.7
	30	$6.63 \cdot 10^{9}$	$6.20 \cdot 10^{9}$	0.374	$6.20 \cdot 10^{-2}$	6.4
SiS-top & CO-bottom	15	$8.65 \cdot 10^{9}$	$7.86 \cdot 10^{9}$	0.184	$8.15 \cdot 10^{-2}$	6.7
SiS-top & O-bottom	30	$5.24 \cdot 10^{9}$	$5.24 \cdot 10^{9}$	0.482	$1.15 \cdot 10^{-1}$	6.2
CO-middle	15	$2.76 \cdot 10^{9}$	$2.90 \cdot 10^{9}$	0.797	0.778	6.7
O-middle	30	$9.70 \cdot 10^{8}$	$1.21 \cdot 10^{9}$	6.79	5.53	5.1
CO-top & He-bottom	15	$8.84 \cdot 10^{8}$	$1.04 \cdot 10^{9}$	2.21	4.72	6.5
O-top & He-bottom	30	$5.00 \cdot 10^{8}$	$6.24 \cdot 10^{8}$	10.2	17.5	5.7
He-middle	15	$2.93 \cdot 10^{8}$	$3.26 \cdot 10^{8}$	18.3	28.9	6.5
	30	$2.90 \cdot 10^{8}$	$3.62 \cdot 10^{8}$	23.2	40.7	5.9
He-top & HeH-bottom	15	$9.75 \cdot 10^{7}$	$1.30 \cdot 10^{8}$	32.2	126	6.9
	30	$1.04 \cdot 10^{8}$	$1.30 \cdot 10^{8}$	19.2	133	7.0

$t/t_u = 2$ the post-shock temperature and density fall typically by a factor of $\sim$5 and $\sim$100, respectively.

Physically, the density-temperature relation at constant entropy $\left(\rho \sim T^{\frac{1}{\Gamma-1}}\right)$ is determined by the adiabatic index Γ that is defined as follows

$$\Gamma = 1 + \left(\frac{\partial \log T}{\partial \log \rho}\right)_S = 1 + \gamma \nabla_A , \quad \text{with} \quad \gamma \equiv \left(\frac{\partial \log P}{\partial \log \rho}\right)_S , \quad \nabla_A \equiv \left(\frac{\partial \log T}{\partial \log P}\right)_S . \qquad (11)$$

Figure 26 shows Γ along isentropes $S = S_p$. We see that Γ is not very different from 4/3 and, therefore, the approximation $\rho \sim T^3$ turns out to be not so far from reality. The exception is the O-shell of a 30 $M_\odot$ model where $\rho \sim T^2$ proves to be a more appropriate approximation since there Γ is close to 1.5 rather than 1.33. Note that at early post-shock times $t/t_u \lesssim 4$, Γ becomes less than 4/3 in the SiS- and CO-shell. This happens owing to the contribution of the electron-positron pairs into the equation of state. For example in the case of a 15 $M_\odot$ model the number of pairs per "atomic" electron is equal to about 0.7 (SiS-middle) and 0.6 (CO-middle) for the peak values of T_p (Table 5) and ρ_p (Tables 1, 5). Thus, the total number of leptons (electrons plus positrons) increases by a factor of ≈ 2.

Conclusion

The approximation formulae presented here, hopefully, seem to be useful for the astrophysicists and nuclear physicists working in the field of stellar nucleosynthesis. In order to adjust their nuclear yields to the supernova models, they have to specify only two basic parameters: radius R_0 and density ρ_0 for a presupernova layer of interest, and to choose the supernova explosion energy E. Then with the Weaver–Woosley temperature $T_{\rm WW}$ (Eq. 2) and characteristic time scale t_u (Eq. 3) known, the temporal behavior of temperature, density, and radius of the Lagrangian layer in question proves to be determined unambiguously by Eqs. (4–6, 8, 9). The corresponding structural coefficients are given in Tables 3 and 4 for a 15 $M_\odot$ and 30 $M_\odot$ supernova, respectively. Although these coefficients are dependent on the supernova mass, the dependence looks not so crucial. In the first rough approximation, one may neglect this dependence assuming the coefficients for a 15 $M_\odot$ model as standard values. In future, it would be worth-while to investigate in details the dependence of the structural coefficients on presupernova mass, metallicity, and stellar rotation.

Acknowledgements

It is a pleasure to express our deep gratitude to the Max-Planck-Institut für Astrophysik for hospitality and financial support. The work was supported also by the Swiss Science National Foundation and the Russian Foundation for Basic Research (Project 00-02-17230).

References

[1] G. Wallerstein, I. Iben Jr, P. Parker et al., Rev. Modern Phys., **69** (1997) 995.

[2] D.K. Nadyozhin, I.V. Panov, A.Yu. Deputovich, in Proceedings of the 10th Workshop on "Nuclear Astrophysics", Ringberg Castle, Tegernsee, Germany, W. Hillebrandt and E. Müller (eds.), **MPA/P12** (2000) 99.

[3] I.Yu. Litvinova, D.K. Nadyozhin, Ap. Sp. Sci. **89** (1983) 89.

[4] S.I. Blinnikov, N.G. Dunina-Barkovskaya, D.K. Nadyozhin, Ap. J. Suppl. **106** (1996) 171.

[5] A.Yu. Deputovich, D.K. Nadyozhin, Pis'ma Astr. Zh. **25** (1999) 750 [Astron. Lett. **25** (1999) 649].

[6] S.E. Woosley, T.A. Weaver, Ap. J. Suppl. **101** (1995) 181.

[7] T.A. Weaver, S.E. Woosley, Ann. NY Acad. Sci. **336** (1980) 335.

[8] F.–K. Thielemann, M. Arnold, W. Hillebrandt, A&A **74** (1979) 175.

[9] D.K. Nadyozhin, I.V. Panov, S.I. Blinnikov, A&A **335** (1998) 207.